MITSUBISHI ELECTRIC RESEARCH LABORATORIES
http://www.merl.com

Channel Measurements of an Indoor Office Scenario for Wireless Sensor Applications

Shurjeel Wyne, Telmo Santos, Fredrik Tufvesson, Andreas Molisch

TR2007-092 August 2008

Abstract

Ad-hoc networks and sensor networks, where nodes communicate with each other without fixed infrastructure, are of great importance for many industrial, environmental, and safety-related applications. The fading statistics of the propagation channels between sensor nodes are essential to determine the possible data rate, outage, and latency of sensor networks. In this paper, we present results from a recent measurement campaign that for the first time provides an in-depth analysis of the propagation channels between typical sensor node locations in office environments. We analyze the Rice factor as a function of distance and find that it is not a monotonically decreasing function. Even in pure LOS situations, Rice factors are on the order of 10 or less. This has important consequences for analysis of bit error rates, diversity order, and diversity/multiplexing tradeoff in clustered sensor networks.

IEEE Global Telecommunications Conference

Channel Measurements of an Indoor Office Scenario for Wireless Sensor Applications

Shurjeel Wyne[1], *Student Member, IEEE,* Telmo Santos[1], *Student Member, IEEE,* Fredrik Tufvesson[1], *Senior Member, IEEE,* and Andreas F. Molisch[1,2], *Fellow, IEEE*

[1]Dept. of Electrical and Information Technology, Lund University, Box 118, SE-221 00 Lund, Sweden.

[2]Mitsubishi Electric Research Labs, 201 Broadway, Cambridge, MA 02139, USA

E-mail: Firstname.Lastname@eit.lth.se

***Abstract*— Ad-hoc networks and sensor networks, where nodes communicate with each other without fixed infrastructure, are of great importance for many industrial, environmental, and safety-related applications. The fading statistics of the propagation channels between sensor nodes are essential to determine the possible data rate, outage, and latency of sensor networks. In this paper, we present results from a recent measurement campaign that for the first time provides an in-depth analysis of the propagation channels between typical sensor node locations in office environments. We analyze the Rice factor as a function of distance and find that it is not a monotonically decreasing function. Even in pure LOS situations, Rice factors are on the order of 10 or less. This has important consequences for analysis of bit error rates, diversity order, and diversity/multiplexing tradeoff in clustered sensor networks.**

I. Introduction

The area of wireless sensor networks has been actively researched in the last few years. A wireless sensor network consists of a number of low-cost low-power sensor nodes, which can perform sensing, simple computation, and communication over short distances [1]. These networks essentially gather information related to the surrounding environment and transmit the data to a nearby sink either directly or via an intermediate node. The indoor scenario is of interest for different sensor applications ranging from security surveillance, inventory management to telemedicine sensors for advanced health care services [2].

The performance of sensor networks, e.g., capacity, reliability, energy consumption, and latency, are all essentially influenced by the statistics of the propagation channels between the sensor nodes. For example, the fading statistics between sensor node pairs determines the routing strategies [3], the amount of cooperation between nodes that is required to achieve a certain outage probability [4], and the optimum placement of sensor nodes [5]. Furthermore, the popular interpretation of clustered sensor networks as virtual MIMO systems critically hinges on the statistics of the propagation channels within each node cluster [6], [7].

Despite this fundamental importance of propagation channel statistics, few measurements of channels between sensor nodes are available. In this paper, we present what we believe is the first systematic measurement campaign for the distance dependence of fading statistics of inter-sensor communications in an indoor environment. The nodes are placed in an office environment, along a wall at 20, 60, and 100 cm above the floor. We show that such a node placement, which is probable in a sensor network, leads to propagation characteristics that are markedly different from the well-studied indoor propagation channel between an access point and a portable device. The measurement frequency is 2.6 GHz, which is close enough to the 2.45 GHz ISM band to yield similar propagation characteristics, but separated enough that the measurements did not suffer from interference from microwave ovens, wireless LANs, etc.

The remainder of the paper is organized as follows. In section II, we discuss the measurement setup and post processing. Section III contains the results and discussion. Finally, we conclude the paper in section IV.

II. Measurement setup and processing

A. Equipment

In our campaign, we measured the transfer function between sensor node antennas at different locations. The data were recorded with the RUSK LUND wideband channel sounder. The measurements were performed at a center frequency of 2.6 GHz and a signal bandwidth of 200 MHz, spanned by 321 spectral lines. The transmit (Tx) signal had a period of 1.6 μs, and an output power of 27 dBm. The propagation channel was measured along designated routes at regular spatial intervals of $\frac{\lambda}{4}$ length, for this purpose a distance triggered signal was provided to the equipment. At each spatial position, a block of ten snapshots was recorded.

The Tx and receive (Rx) antennas were Skycross (SMT-2TO6M-A) meander line antennas with linear polarization, dimensions $2.8 \times 2.2 \times 0.3$ cm^3. The antenna pattern was measured prior to conducting channel measurements, refer Fig. 1; the azimuth pattern (in the plane perpendicular to axis of the antenna) was omnidirectional whereas the elevation pattern contained some radiation lobes.

B. Scenario

The measurements were performed in the E-building at LTH, Lund, Sweden in three office rooms, each of dimension 6×3

1930-529X/07/$25.00 © 2007 IEEE

This full text paper was peer reviewed at the direction of IEEE Communications Society subject matter experts for publication in the IEEE GLOBECOM 2007 proceedings.

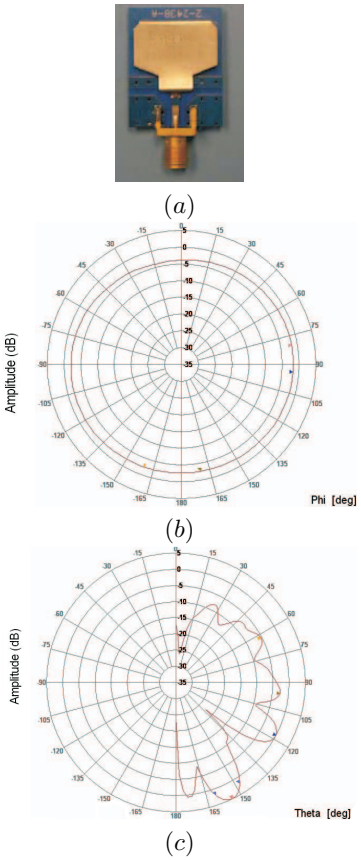

Fig. 1. a) Rx and Tx antenna (b) Azimuth (c) Elevation Pattern.

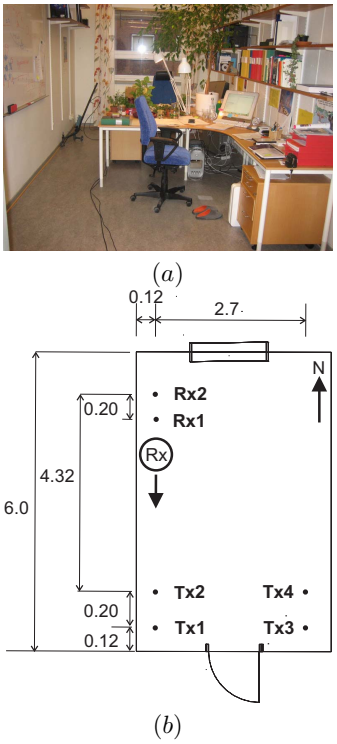

Fig. 2. (a) Room 2364, window on North wall. (b) Measurement plan.

m^2. The measurement layout is shown in Fig. 2. Measurements were conducted at three sets of equal antenna heights, i.e., Tx and Rx antennas both maintained at 20 cm above floor, referred to as Tx20Rx20 configuration. Similarly a Tx60Rx60 and Tx100Rx100 configuration was also used in the measurements. The following description applies to each height configuration; In every room 6 measurement runs were performed corresponding to each of the two 6 m walls. In every run the Rx antenna was moved along the 6 m wall such that in runs 1 and 2 the stationary Tx antenna was placed along the opposite 6 m wall, in runs 3 and 4 the Tx antenna was placed along the same wall as the Rx, in runs 5 and 6 the "same-wall" measurement was repeated but with both antennas tilted 90 degrees so that the azimuth pattern became the uniform elevation pattern (UEP). The full set of measurements was repeated for the other 6 m wall so that in total 108 distance triggered runs were measured over the 3 rooms and 3 height configurations. Note that the maximum and minimum Tx-Rx separation for the same-wall case are 4.3 m and 0.17 m, respectively.

Though we have investigated all measurements, for space reasons we present here results only for the 36 UEP same-wall measurements. Choosing an antenna pattern that is uniform in elevation allows an accurate characterization of the floor reflections[1]. As we will see later on, the received power is critically influenced by the floor reflections. Furthermore, the reflections change with the distance between Tx and Rx, since the floor appears in different Fresnel ellipsoids for different antenna heights and Tx-Rx distances used in the measurement.

C. Data Post Processing

The measured signal to noise ratio was always in excess of 20 dB. A further 10 dB improvement in SNR was achieved by coherent averaging of complex channel gains over 10 snapshots recorded per spatial sample. To analyze the small-scale fading statistics a measurement run was divided into 7 non-overlapping segments, each consisting of 20 adjacent spatial samples[2] separated by $\frac{\lambda}{4}$. Each of these $4\frac{3}{4}\lambda$ length segments was treated as a small-scale area (SSA). Furthermore, the sampled channel transfer functions within a segment were used as statistical ensemble for the narrowband path gains, h_{ij}. For small-scale analysis, the path gains were normalized so as

[1]For the different height-above-floor measurements, antenna-to-wall separation was maintained at 12 cm. At this separation, the azimuth pattern is assumed to be the same for direct and wall-reflected components in the UEP case.

[2]The number 20 comes from a trade-off between two conflicting requirements, i.e., to have sufficient statistical samples; and the necessity, by definition of a small-scale region [8], to have negligible variation in the mean Rx power. See also the discussion later in this section.

to remove distance dependence and large-scale variations,

$$h_{\mathrm{ij}}^{\mathrm{norm}} = \frac{h_{\mathrm{ij}}}{\sqrt{\frac{1}{20F}\sum_{i=1}^{20}\sum_{j=1}^{F}|h_{\mathrm{ij}}|^2}}, \quad (1)$$

where F is the number of spectral lines in the signaling bandwidth and $\frac{1}{20}\sum_{i=1}^{20}(\cdot)$ represents a sliding-window average of the received power along a measurement run. The effect of normalization at different antenna heights is shown in Fig. 3. It can be observed that for the Tx20Rx20 configuration there is residual variation in mean Rx power over the small-scale segment closest to Tx, the corresponding effect on small-scale statistics will be discussed in Sec. III-A.2.

The statistics for each SSA were investigated using an ensemble size of 20×321 samples. The 321 samples in the frequency domain were not all independent, as confirmed by the coherence bandwidth which was observed to be on the order of 12 MHz. We can conclude that around 17 statistically independent samples were available in the frequency domain. For each of the 7 SSA ensembles, we use the computed value of the Rician K-factor as a metric to decide whether a Rician or Rayleigh distribution appropriately describes the measured statistics, see Sec. III-A.1 for details.

We note that the number of statistically independent samples in a SSA is relatively low, and may lead to uncertainties in the estimated parameters. However, the limits to the sample number are inherent in the analyzed scenario, and cannot be eliminated by increasing length of the SSA or measurement bandwidth:

(i) Increasing the length of the SSA: The SSA segment of length $4\frac{3}{4}$ wavelengths is smaller than the $10-20$ λ that are commonly used as SSA window length. This window size was selected empirically[3] with the consideration that the mean Rx power should not exhibit a distance-dependence over the length of the window. In this respect, the SSA closest to the Tx is potentially the worst case; the free-space model predicts 13 dB variation in mean Rx power between it's end-points. However, our measurements for such an SSA show that though the Rx power fluctuates due to the influence of floor and wall reflections, there is clearly no distance dependence. To further verify absence of free-space (distance-dependent) path-loss from this SSA, we normalized the small-scale ensemble to remove free-space loss. The Rician K-factor, which is a measure of small-scale variations, was practically unchanged when computed before and after this normalization.

(ii) Increasing the measurement bandwidth: this approach would lead to a larger number of independent samples; but is not only difficult to implement, but also faces fundamental problems. When the measurement bandwidth exceeds 10 - 20 % of the carrier frequency, the channel statistics are not identical in the different sub-bands of the measurement spectrum anymore [9]. In other words, the uncorrelated-scattering assumption of [10] is violated.

In the sequel, we present statistics for small-scale coherence distance. Our investigations on synthetic data[4] show that it is sufficient to use 100 statistical samples for each lag to get an accurate autocovariance estimate, refer to Fig. 4. For the measurements, we compute the autocovariance at each spatial-lag of interest, using 10 spatial samples and the frequency domain realizations. With a median coherence bandwidth of 12 MHz, this means that on average we have used 170 independent statistical samples per lag to estimate the small-scale distance correlation.

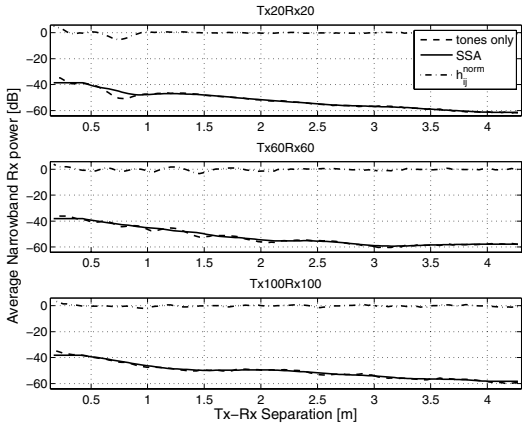

Fig. 3. Narrowband Rx power vs distance, averaged over 12 UEP same-wall measurements. For the "tones only" curve, the narrowband power in each run was averaged over bandwidth. For the "SSA" curve, the Rx power in each run was averaged over a sliding window of 20 samples. The normalized channel refers to Eq. (1). Antenna heights are indicated above each subplot.

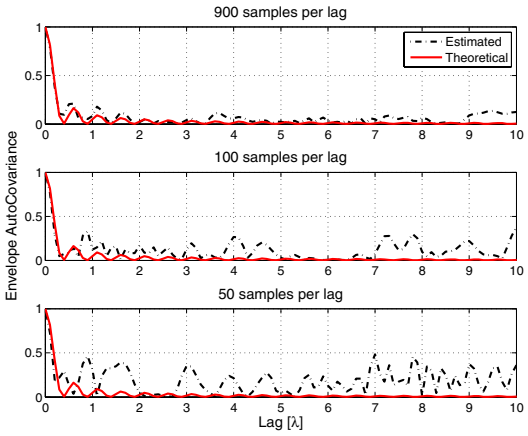

Fig. 4. Estimated autocovariance of synthetic Rayleigh envelope samples. The subplots show how number of independent statistical samples influences accuracy of estimation. The theoretical autocovariance (squared Bessel function of zero-th order) is also shown for reference.

[3]After comparing various lengths of the averaging window for different measurement routes.

[4]Rayleigh distributed envelope samples were generated with an autocovariance given by the squared zero-th order Bessel function.

1930-529X/07/$25.00 © 2007 IEEE

III. Results

A. Small-Scale Statistics

1) Envelope Distribution: In our measured scenarios, the small-scale distribution of the narrowband envelope is modeled as either Rician or Rayleigh. This choice of distributions comes from the scenario under consideration, i.e., unobstructed line of sight between Tx and Rx. Furthermore, with this choice of distributions, we also investigate if a well-defined transition occurs from Rayleigh to Rice with decreasing Tx-Rx distance as considered in other published work [6]. In our analysis the Rician K-factor[5], K_{Rice}, is used as a metric to determine the small-scale envelope distribution. Similar to the analysis in [12], a Rayleigh statistic is decided when $K_{\text{Rice}} \leq 1$, i.e., the estimated power in the deterministic component of the channel is less than or equal to estimated power in the random component. The envelope distribution is considered to be Rician in all other cases. When transmitter and receiver are on the same wall, the envelope distribution was observed to be Rician in most cases, though large values ($K_{\text{Rice}} > 10$) are observed only for Tx20Rx20, refer Fig. 5. We also observed that in comparison to the other antenna heights, the Tx20Rx20 configuration had less occurrences that the Rayleigh distribution was a good fit to the measurement data. For the opposite wall measurements (not presented in this paper), a Rayleigh distribution was frequently observed to fit the measured envelope distribution.

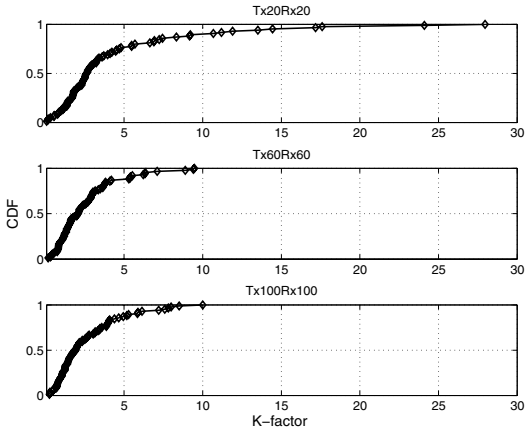

Fig. 5. CDF of K_{Rice} for the same-wall UEP measurements. Height of antenna is given above each subplot. All K-factors are on a linear scale.

In Fig. 6 the envelope distribution is shown for small-scale segments belonging to one measurement run. While in most cases the Rice distribution provides an excellent fit to the measured envelope pdf, in some segments the envelope distribution does not retain it's strong Rician characteristics. This is a sign that for those segments, the underlying signal model that is based on the validity of the central limit theorem, might not be valid for the considered situation. A number of alternative small-scale distributions has been proposed in the literature, including the Nakagami and Weibull distributions [8], in particular the Nakagami-m has been used in similar scenarios [13]. Choosing which of these distributions fits the data best could be done by information-theoretic criteria [14]. However, a comparative study is not done here due to space constraints.

[5]Rice factors were computed from the moment method of [11].

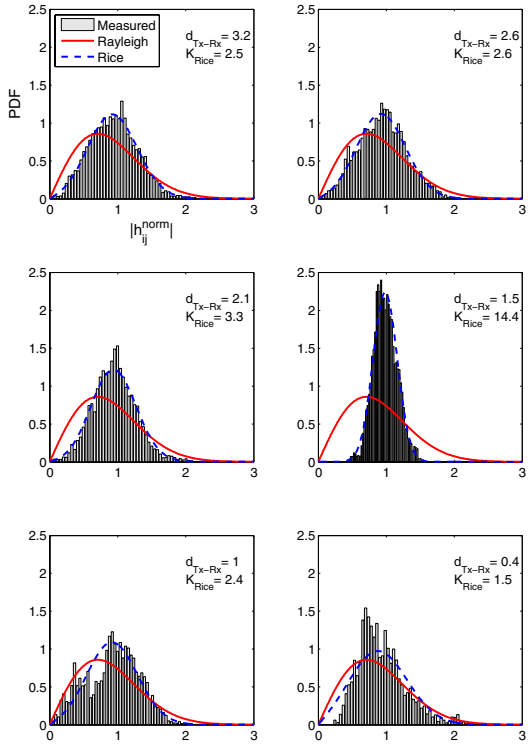

Fig. 6. Small scale envelope distribution along one measurement run (Tx20Rx20). Each subplot represents one SSA; the parameter $d_{\text{Tx-Rx}}$ for each subplot is the distance from center of respective SSA to Tx. K_{Rice} is the Rician K-factor estimated from measurements. The Rice and Rayleigh curves are also shown for reference.

2) Rician K-factor: Theoretical studies on communication between clusters of sensor nodes often make simplifying assumptions about the propagation channels between the nodes. The two most popular models are (i) Rayleigh fading between *all* nodes, independent of the distance between them, (ii) Additive White Gaussian Noise (AWGN) or equivalently Rician fading with high K-factor for nodes communicating within a cluster, i.e., small Tx-Rx separation, and Rayleigh fading between nodes belonging to different clusters. It also seems intuitively pleasing that the Rice factor would increase as the separation between Tx and Rx decreases, and eventually reach very high values for small separations. However, our measurements show quite different trends - there is no monotonic increase in K-factor with decreasing distance.

Fig. 7 shows the mean K-factors plotted as a function of Tx-Rx separation. The fluctuation in K-factor along the measurement run is seen at all three heights. The Tx20Rx20 curve, in particular, dips to a low value at small distances. This dip is explained from Fig. 3 which shows, for Tx20Rx20, small-

TABLE I

REGRESSION PARAMETERS FOR MEAN K-FACTOR (LINEAR SCALE).

Antenna height	$P(x) = a_3x^3 + a_2x^2 + a_1x + a_0$				Variance
	a_3	a_2	a_1	a_0	
Tx20Rx20	1.13	-9.31	21.26	-6.80	3.82
Tx60Rx60	-0.05	0.72	-2.88	5.52	0.20
Tx100Rx100	-0.25	1.7	-3.83	5.401	0.09

scale variations over the segment closest to Tx. As shown in Fig. 7, a cubic polynomial has been used to model K-factor variations along a measurement run. The regression parameters are provided in Table. I. The curve fitting suggests that a lower degree polynomial may also be used for the Tx60Rx60 and Tx100Rx100 configurations.

A "sanity check" of the measurements can be obtained with a theoretical 3-path model that extends the standard 2-path model [8] to include a wall reflection. In the 3-path model, the total electric field is deterministic and is the vector sum of the direct component and the two reflections. The squared magnitude of the total electric-field, i.e., power of the deterministic component, is plotted in Fig. 8. The electric-field values have been scaled to remove distance dependence, which is conventional practice in small-scale analysis of channel coefficients. Under the simplifying assumption that the 3-path channel now admits a scattering component with constant mean power, the plot in Fig. 8 is a measure of the Rician K-factor along the measurement run. Some resemblance to our measurements can be observed. We find that also in the synthetic scenario, there is variation in the K-factor due to interference of the dominant deterministic components. A peak is observed around 1.5 m Tx-Rx separation. However, at very close Tx-Rx separation our measured results diverge from the synthetic channel. This can be attributed to our selection of SSA length of 20 spatial samples which smooths out the interference effects at small separations. The practical considerations that motivate this SSA length have already been discussed in Sec. II-C.

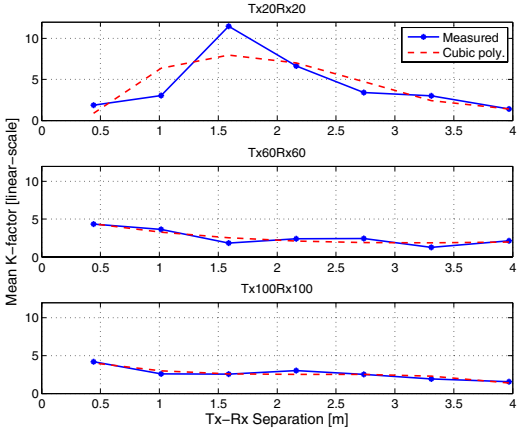

Fig. 7. Variations of mean K-factor along a measurement run. The mean is calculated over 12 UEP same-wall measurements.

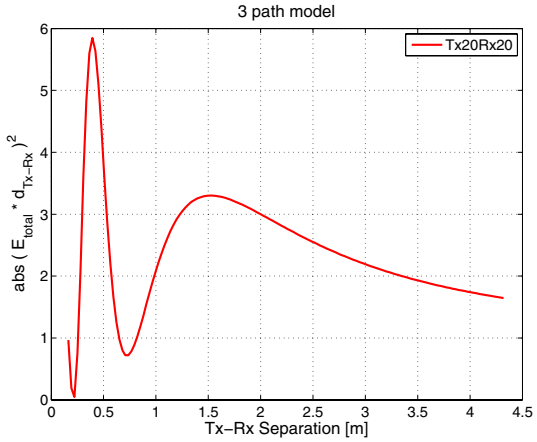

Fig. 8. Distance-scaled Rx power for a 3-path model. The Tx and Rx antennas are assumed to be isotropic radiators maintained at 20 cm height above floor and 12 cm wall separation. Reflection from the wall and floor is assumed to be lossless.

3) Envelope Autocovariance: The autocovariance of the envelope is commonly used to characterize the spatial selectivity of the channel. We define the normalized autocovariance of the envelope process as

$$\rho_{xx}(\Delta d) = E\left[\frac{X_i - E[X_i]}{\sqrt{var(X_i)}} \cdot \frac{X_{i+\Delta d} - E[X_{i+\Delta d}]}{\sqrt{var(X_{i+\Delta d})}}\right], \quad (2)$$

where the expectation is taken over the channel samples normalized according to Eq. (1). When estimating the autocovariance according to Eq. (2), an equal number of statistical samples have been used for each lag. The maximum considered lag corresponds to a separation of 10 intervals of length $\frac{\lambda}{4}$ between envelope samples. From the normalized autocovariance plot, the decorrelation distance is defined as

$$d_{\text{de-corr}} = \min\{\Delta d : \rho_{xx}(\Delta d) \leq 0.7\}.$$

The distribution of decorrelation distance at different antenna heights is shown in Fig. 9. It can be inferred from the plots that the decorrelation distances for small-scale fading, as measured along a wall, are on the order of $\frac{1}{2}$ wavelength.

B. Large-Scale Characteristics

The average large-scale pathloss is conventionally modeled as a power law decay with distance, where the rate of decay is parameterized by the pathloss exponent. In our individual measurement runs, the small-scale fading is removed by averaging the narrowband Rx power over a sliding window of length 20 spatial samples. The mean of these Rx power vs. distance curves, taken over 12 same-wall measurements, gives the "measured" curves in Fig. 10. We have performed a regression analysis on these curves and the regression parameters are provided in Table. II. From the tabulated values, the pathloss exponent is close to 2 for all three heights. Also, the standard deviation which is a measure of large scale fading is very similar for the three heights.

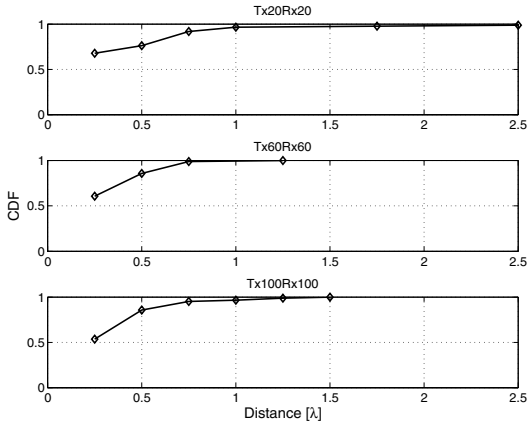

Fig. 9. Distribution of the decorrelation distance for small scale fading. Decorrelation is defined as $\rho_{xx}(\Delta d) \leq 0.7$. Antenna heights are indicated above each subplot.

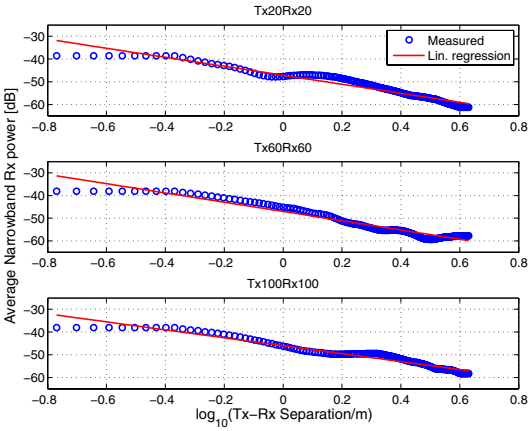

Fig. 10. Large-scale variations of Rx power along measurement run. The horizontal axis is the logarithm of Tx-Rx distance in meters.

IV. Summary and Conclusions

In this paper we have presented results for selected parts of our indoor office measurements for sensor networks. We have characterized, for three different heights, the scenario when Tx and Rx antenna are located along the same wall. Our results show that the small-scale envelope distribution is mostly Rician, though the K-factors are not very large. Our measurements indicate that the K-factor does not increase monotonically as the Tx-Rx distance is reduced, this result is contrary to the widely accepted assumption in published literature; that the channel is AWGN at a small-enough distance. We provide the regression parameters for a cubic fit to our measured K-factors. We have investigated the small-scale spatial selectivity of the channel and show that the decorrelation distance is on the order of $\frac{1}{2}$ wavelengths. Our analysis of the large-scale variations of Rx power show that the pathloss exponent is close to 2 and the large-scale fading is very similar for the three antenna heights measured in the same-wall scenario. Our results are relevant to communicating within, and between, clusters of nodes and have practical significance because in realistic indoor scenarios the sensors will often be deployed in close proximity to the wall and floor. Strong (but not Rayleigh) fading will occur even between links that have good line-of-sight connection. This means that communication between nodes in a cluster cannot occur with complete reliability, and that the distribution of Rice factors has to be taken into account, in order to arrive at realistic evaluations of the diversity/multiplexing trade-off in ad-hoc networks.

TABLE II

REGRESSION PARAMETERS FOR LARGE SCALE FADING.

Antenna height	$P(x) = a_1 x + a_0$		STD [dB]
	a_1	a_0	
Tx20Rx20	-19.8	-47.2	1.6
Tx60Rx60	-20.5	-47.0	1.6
Tx100Rx100	-17.5	-46.0	1.3

V. Acknowledgements

This work was partly financed by High Speed Wireless Center and INGVAR grants of the Swedish Foundation for Strategic Research, and a grant from Vetenskapsrådet, the Swedish Science Council. We would like to thank Perlos AB, Lund, for facilitating the antenna pattern measurements.

References

[1] A. Willig, K. Matheus, and A. Wolisz, "Wireless technology in industrial networks," *Proceedings of the IEEE*, vol. 93, no. 6, pp. 1130–1151, 2005.

[2] I. Akyildiz, T. Melodia, and K. Chowdhury, "A survey on wireless multimedia sensor networks," *Computer Networks*, vol. 51, pp. 921–960, October 2007.

[3] J. Al-Karaki and A. Kamal, "Routing techniques in wireless sensor networks: a survey," *IEEE Wireless Communications Magazine*, vol. 11, pp. 6–28, December 2004.

[4] A. F. Molisch, N. B. Mehta, J. Yedidia, and J. Zhang, "Cooperative relay networks using fountain codes," in *Proc. IEEE Globecom 2006*, (San Francisco, USA), November/ December 2006.

[5] E. L. Lloyd and G. Xue, "Relay node placement in wireless sensor networks," *IEEE Transactions on Computers*, pp. 134–138, January 2007.

[6] M. Yuksel and E. Erkip, "Diversity gains and clustering in wireless relaying," *Information Theory, 2004. ISIT 2004. Proceedings. International Symposium on*, p. 402, 2004.

[7] M. Yuksel and E. Erkip, "Cooperative wireless systems: A diversity-multiplexing tradeoff perspective," *submitted to IEEE Transactions on Information theory*, 2007.

[8] A. F. Molisch, *Wireless Communications*. IEEE Press - Wiley, 2005.

[9] A. F. Molisch, "Ultrawideband propagation channels-theory, measurement, and modeling," *IEEE Transactions on Vehicular Technology*, vol. 54, no. 5, pp. 1528–1545, 2005.

[10] P. A. Bello, "Characterization of randomly time-variant linear channels," *IEEE Transactions*, pp. 360–393, December 1963.

[11] L. J. Greenstein, D. G. Michelson, and V. Erceg, "Moment-method estimation of the Ricean K-factor," *IEEE Communications Letters*, vol. 3, pp. 175–176, June 1999.

[12] H. Asplund, A. A. Glazunov, A. F. Molisch, K. Pedersen, and M. Steinbauer, "The COST 259 directional channel model part II: Macrocells," *IEEE Transactions on Wireless Communications*, vol. 5, no. 12, pp. 3434–3450, 2006.

[13] A. Adinoyi and H. Yanikomeroglu, "Cooperative relaying in multi-antenna fixed relay networks," *IEEE Transactions on Wireless Communications*, pp. 533–544, February 2007.

[14] U. G. Schuster, H. Bolcskei, and G. Durisi, "Ultra-wideband channel modeling on the basis of information-theoretic criteria," *Information Theory, 2005. ISIT 2005. Proceedings. International Symposium on*, pp. 97–101, 2005.